

ARTICLES

Laser Ablation Synthesis of Spindle-like Gallium Oxide Hydroxide Nanoparticles with the Presence of Cationic Cetyltrimethylammonium Bromide**Chih-Chia Huang and Chen-Sheng Yeh****Department of Chemistry, National Cheng Kung University, Tainan 701, Taiwan***Ching-Jeng Ho****Department of Mechanical Engineering, National Cheng Kung University, Tainan 701, Taiwan**Received: November 11, 2003; In Final Form: February 19, 2004*

Laser ablation of gallium metal was performed to prepare spindle-like GaOOH particles in aqueous solution. Formation of well-defined GaOOH was strongly associated with the addition of cationic CTAB surfactant. It was found that spindle-like GaOOH could be grown in below, near, or above critical micelle concentrations (cmc) of CTAB via an aging process. On the other hand, using anionic SDS surfactant or pure H₂O solvent could not exclusively give the final spindle-like GaOOH, but the irregular and amorphous materials were produced. TEM, XRD, FT-IR, SEM, XPS, ζ -potential, and ¹H NMR measurements were carried out to characterize the resulting precipitates. High-resolution TEM indicated that GaOOH crystals formed a type of layered structure and grew along the $\langle 001 \rangle$ axis. Without the presence of the surfactants, the nascent colloidal solutions, immediately after laser ablation, were prepared for the ζ -potential measurements. The negative sign of ζ -potential for the laser-ablated surfactant-free colloids indicates that the cationic CTAB would preferentially adsorb onto the colloidal negative surface. It is proposed that the adsorption of the CTAB might have facilitated the development of the ellipsoidal nanocrystals through a slow crystallization process. Calcination of these gallium oxide hydroxides at a temperature of 750 °C (18 h) transformed into β -Ga₂O₃, but following a stepwise pathway, i.e., 250 °C (64 h) \rightarrow 250 °C (64 h) \rightarrow 750 °C (18 h), converted as α -Ga₂O₃.

Introduction

Nanoscale materials have been demonstrated to exhibit novel characteristics in optical, catalytic, and magnetic applications. Diverse metal and metal oxide nanostructures could be prepared using either chemical or physical approaches. Laser ablation is an approach that provides an efficient route to readily generate nanometer colloids. Nanosecond or femtosecond laser ablation of the metal surfaces or the metal powders in the liquid was employed to prepare metal and alloy colloidal suspensions.^{1–15} In addition, we have demonstrated that laser irradiation of an Al rod immersed in H₂O followed by a course of aging led to the formation of aluminum hydroxide particles with bayerite, gibbsite, and boehmite polyforms.^{9,10}

Monoclinic gallium oxide (β -Ga₂O₃) has been known to exhibit both the properties of conduction and luminescence.^{16–18} It is a transparent conducting oxide and can be applied as an optoelectronic device.^{19,20} There is no doubt that nanoscale gallium-based materials might present distinctive behavior, which may find useful applications for mini-devices. Unfortunately, few attempts were devoted to synthesizing gallium oxide-based nanostructures. Recently, arc discharge¹⁷ and laser ablation combined with a high temperature-furnace¹⁸ have been successfully employed to grow β -Ga₂O₃ nanowires. Gedaken and

co-workers, using sonochemical reduction, produced scroll-like layered gallium oxide hydroxide (GaOOH).²¹ Tas and co-workers prepared nanometer or micrometer GaOOH particles by using either homogeneous decomposition of urea or forced hydrolysis in pure water, respectively.²² Tas et al. showed that as-synthesized GaOOH, following calcination at 500 °C, resulted in rhombohedral Ga₂O₃ (α -Ga₂O₃), and the monoclinic Ga₂O₃ (β -Ga₂O₃) was attained for the calcination temperature above 750 °C.

We have prepared AlOOH colloidal particles by laser ablation of an Al rod immersed in H₂O without additives.^{9,10} Building on those studies, we here irradiated a Ga target in H₂O by a pulsed nanosecond laser, leading to spindle-like (ellipsoid-like) GaOOH nanoparticles. Interestingly, the ellipsoidal GaOOH can only be observed with the presence of cationic cetyltrimethylammonium bromide surfactant. Contrary to the results of Tas et al. that calcination of GaOOH transformed as α -Ga₂O₃ at 500 °C and as β -Ga₂O₃ at a temperature of 750 °C,²² the pathway of the elevated temperature up to 750 °C determined the formation of either α -Ga₂O₃ or β -Ga₂O₃ from the resulting ellipsoidal GaOOH.

Experimental Section

Laser ablation was performed by placing a gallium plate (>99.9%, 1.5 cm \times 1 cm) on the bottom of a Pyrex vial filled with 4 mL of solvent. The experimental conditions with the

* Authors to whom correspondence should be addressed. E-mail: csyeh@mail.ncku.edu.tw; cjho@mail.ncku.edu.tw.

solvent of choice were an aqueous solution of cationic cetyltrimethylammonium bromide (99+%, Acros; denoted as CTAB hereafter), of anionic dodecylsulfuric acid sodium salt (>95%, Tokyo Kasei Kogyo Co. Ltd.; denoted as SDS hereafter), and of pure water. With the presence of anionic or cationic surfactants, the surfactants were adjusted to the concentrations of below, near, and two times their critical micelle concentrations (cmc). The cmc values are $\sim 8.3 \times 10^{-3}$ M for SDS and $9.0\text{--}9.8 \times 10^{-4}$ M for CTAB.²³

An unfocused Nd:YAG laser (Quantel Brilliant) operated at 10 Hz (5 ns pulse width) with a wavelength of 1064 nm was utilized to irradiate a Ga plate immersed in solvent. In general, laser intensity of 100 mJ/pulse was employed to ablate a metal plate with irradiation duration of 20 min. All manipulations were carried out in an aerobic condition.

Electron micrographs using transmission electron microscopes (Hitachi FE-2000 and Zeiss 10c) were attained by placing a drop of the sample on a copper mesh coated with an amorphous carbon film, followed by evaporation of the solvent in a vacuum desiccator. Scanning electron microscopic (SEM) images of the ellipsoidal GaOOH on a copper substrate were carried out with a Hitachi S4200 field emission scanning electron microscope. XRD data were collected on a Rigaku D-Max III/V diffractometer using Cu K α radiation ($\lambda = 1.54056$ Å) at 30 kV and 30 mA. All XP spectra were recorded using a Mg K α source (12 kV and 10 mA). The binding energy scale was calibrated to 284.6 eV for the main (C 1s) peak. Fourier transform infrared spectra using a KBr disk dispersed with the powder sample were measured with a Nicolet Avatar 360 for the analysis of the resulting samples. The solution ¹H NMR spectra were obtained using a Bruker AVANCE 300 FT-NMR spectrometer. Gas chromatography was analyzed by using VG 70-250S spectrometer. The ζ -potential of the native colloidal solution without the presence of the surfactants was measured using a Zetasizer analyzer (Malvern, UK).

Results and Discussion

Laser ablation of Ga metal was conducted in the aqueous solutions of CTAB and SDS, and of pure water. It was found that the spindle-like GaOOH nanoparticles were well-formed in the presence of CTAB surfactant. In addition, the ellipsoidal GaOOH formation by following the aging course can be observed under the CTAB concentrations where they are below (5.5×10^{-4} M), near (1.1×10^{-3} M), and above (2.2×10^{-3} M) cmc. The samples prepared from 2.2×10^{-3} M solution were selected as the typical results throughout the text. As laser irradiation for 20 min, the nascent solution appeared as transparent with a slight yellowish color. The final temperature of the solution rose by ca. 6 °C from the initial solvent temperature (20–21 °C). Following an aging process, the solution became slightly turbid, accompanied by fluffy coagulation after 3 h. The pale aggregates increased as aging was prolonged. TEM images of Figure 1 show the formation of GaOOH particles from the nascent product to the solution aged for 7 days.

At the beginning, the laser-ablated solution manifested in a state of agglomeration and contained an amorphous material, as shown in Figure 1a. Interestingly, Figures 1b,c show that the fluffy aggregates developed as ellipsoid-like morphology after aging 1 and 7 days. As the aging time lengthened to 7 days, the ellipsoidal precipitates increased and their dimensions grew. Although the grown particles have a large deviation in sizes, the average ellipsoidal dimensions basically increased from 216.9 ± 97.7 nm (1 day) to 314.2 ± 119.8 nm (7 days) in

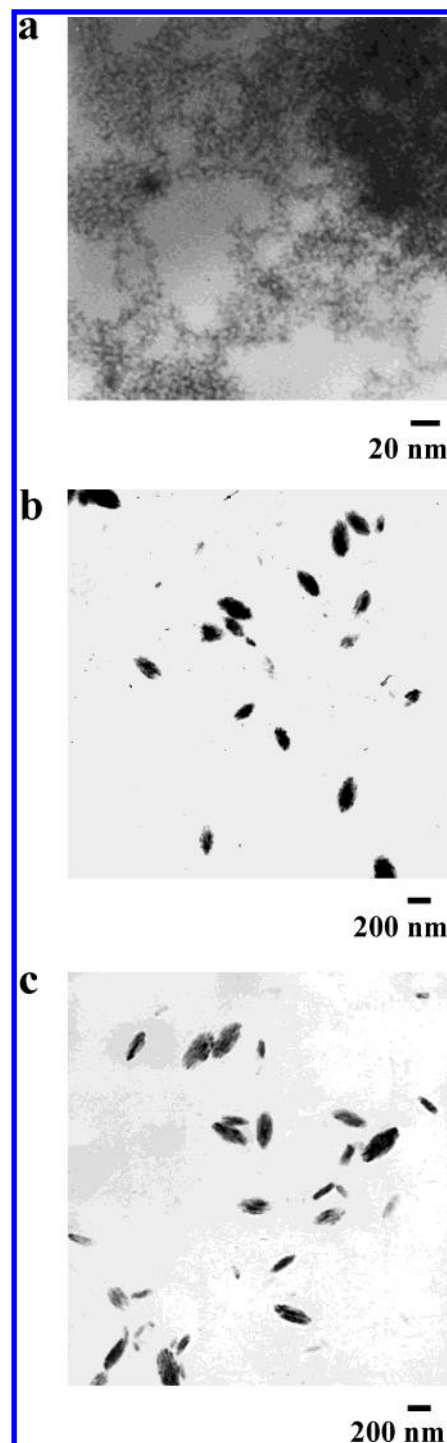


Figure 1. TEM images attained under the 2.2×10^{-3} M CTAB with laser operation by a 1064 nm wavelength using 100 mJ/pulse for a 20 min irradiation time: (a) the nascent species immediately after laser ablation; (b) the spindle-link particles after aging 1 day; (c) the grown spindle-link particles after aging 7 days.

length and 103.1 ± 52.9 nm (1 day) to 139.2 ± 74.5 nm (7 days) in width. We have also inspected products which have a 14-day aging period. The dimensions in length (304.2 ± 88.1 nm) and width (114.3 ± 47.3 nm) seemed to indicate that the particles ceased growing. As mentioned earlier, three different CTAB concentrations, i.e., 5.5×10^{-4} M, 1.1×10^{-3} M, and 2.2×10^{-3} M, can all form such ellipsoidal structures. The particle dimensions exhibited a trend of enlargement as CTAB concentrations increased. For example, the ellipsoidal dimensions lengthened from 214.3 nm (5.5×10^{-4} M) to 304.2 nm (2.2×10^{-3} M) measured from the products after aging 14 days.

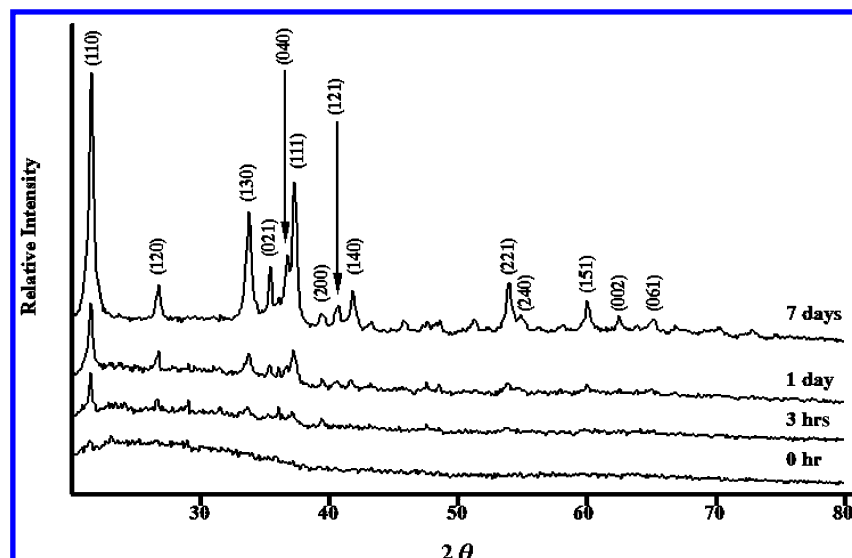


Figure 2. Development of XRD patterns as a function of aging period. A 1064 nm wavelength with laser intensity of 100 mJ/pulse was employed to irradiate a gallium plate in an aqueous solution of 2.2×10^{-3} M CTAB for 20 min exposure time.

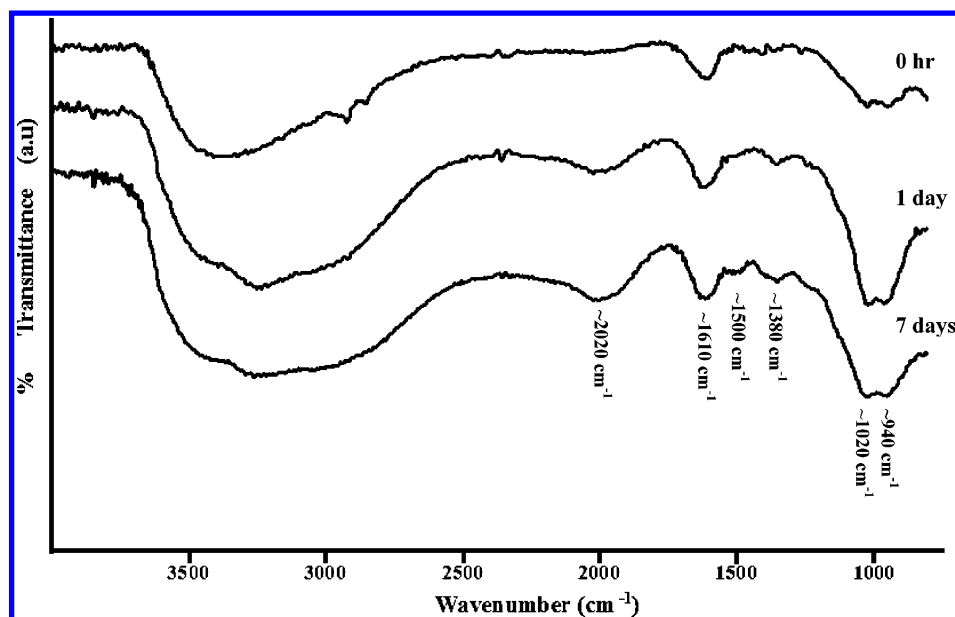


Figure 3. Development of FT-IR spectra as a function of aging period. A 1064 nm wavelength with laser intensity of 100 mJ/pulse was employed to irradiate a gallium plate in an aqueous solution of 2.2×10^{-3} M CTAB for 20 min exposure time.

Prior to preparing a TEM sample, the aged precipitates were all sonicated in a few minutes via an ultrasonicated cleaner (70 W) for the purpose of dispersing the precipitates in the solvent. Because a laser was employed to prepare particles, ^1H NMR was used to inspect any side reaction product other than gallium-based particles. Following the centrifugation, the resulting supernatants were studied by ^1H NMR. ^1H NMR verified no species but CTAB molecules existed in solutions. In addition, gas chromatography was also introduced to examine supernatants and detected no byproducts. For the effect of the laser fluence in forming a spindle-like structure, a lesser laser fluence with 50 mJ/pulse was introduced to ablate the metal plate with an irradiation time of 20 min in 2.2×10^{-3} M of CTAB as well. It was found that the ellipsoidal particles also can be observed after aging 1 day. However, a significantly decreased amount of particles was generated and possibly was due to much fewer particle embryos available by a laser ablation with smaller laser power.

XRD measurements were performed to investigate laser-ablated products. Figure 2 shows the development of the XRD

patterns as a function of aging duration. It is apparent that XRD diffraction peaks grew gradually as aging time was prolonged. Those arisen peaks can be identified and were characterized as belonging to gallium oxide hydroxide (GaOOH) crystals. From XRD results, we also noticed that the nascent solution, immediately after ablating, contained a structureless material. The IR spectra present the precipitates prepared from CTAB solutions and aged for a set period of time, as shown in Figure 3. The collected samples were dried using a vacuum oven (NAPCO 5831) operated at 80 °C before measuring IR spectra. A broad band appeared above 2600 cm^{-1} and significantly became intense with increasing aging time. It is known that an H—O—H stretching band appears at around 3400 cm^{-1} and O—H stretching of GaOOH emerges at 3200 cm^{-1} .^{22,24} In fact, the IR contour clearly demonstrated that the band position enhanced and shifted from ~ 3400 to $\sim 3200\text{ cm}^{-1}$ as GaOOH gradually grew. An additional band at $\sim 1610\text{ cm}^{-1}$ can be observed in all sample sets and is assigned to the bending mode of H_2O . The spectra in Figure 3 also contain bands at ~ 1020 and $\sim 940\text{ cm}^{-1}$; they also have bands at $\sim 2020\text{ cm}^{-1}$ due to

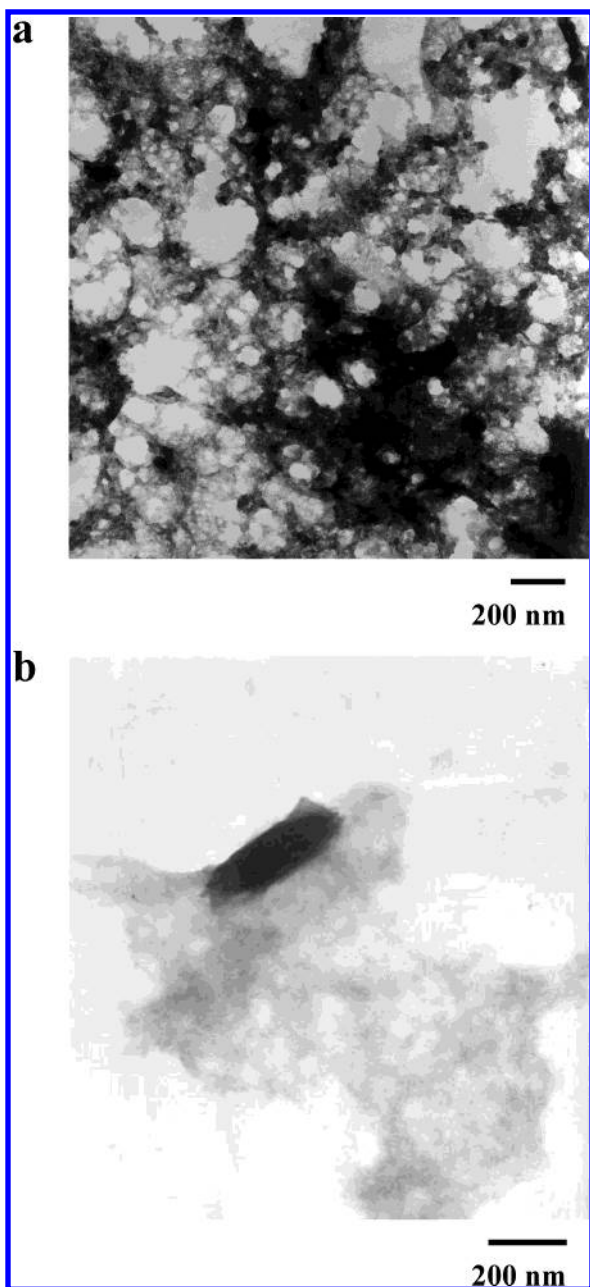


Figure 4. TEM image of the resulting products prepared by a 1064 nm wavelength using 100 mJ/pulse for a 20 min irradiation time, followed by aging 7 days: (a) with 1.0×10^{-2} M of SDS, (b) pure H_2O .

the Ga—OH bending mode of GaOOH and its overtones, respectively.^{22,24} Most interestingly, such a Ga—OH bending band can be determined as early as in those nascent products. Together with XRD results, it is suggested that the precipitates transformed amorphous hydroxide containing gallium into well-grown GaOOH crystals during aging. Due to addition of CTAB in the preparation solution, it is reasonable to expect the appearance of the relevant CTAB bands. Based on the literature values, the asymmetric and symmetric deformation modes pertaining to $\text{CH}_3\text{—N}^+$ of the CTAB headgroup appear at ~ 1490 and $\sim 1390\text{ cm}^{-1}$, respectively.²⁵ Although our results indicated the signals of two bands at ~ 1500 and $\sim 1380\text{ cm}^{-1}$, poor signal-to-noise cannot provide as strong evidence for the CTAB molecules accompanied with GaOOH. To further verify the characteristic in the CTAB, the XPS analysis was carried out to determine nitrogen signal. The $\text{N}(1s)$ binding energies were determined to be 397.9, 397.2, and 397.9 eV for the aged precipitates of 0 h, 1 day, and 7 days, respectively.

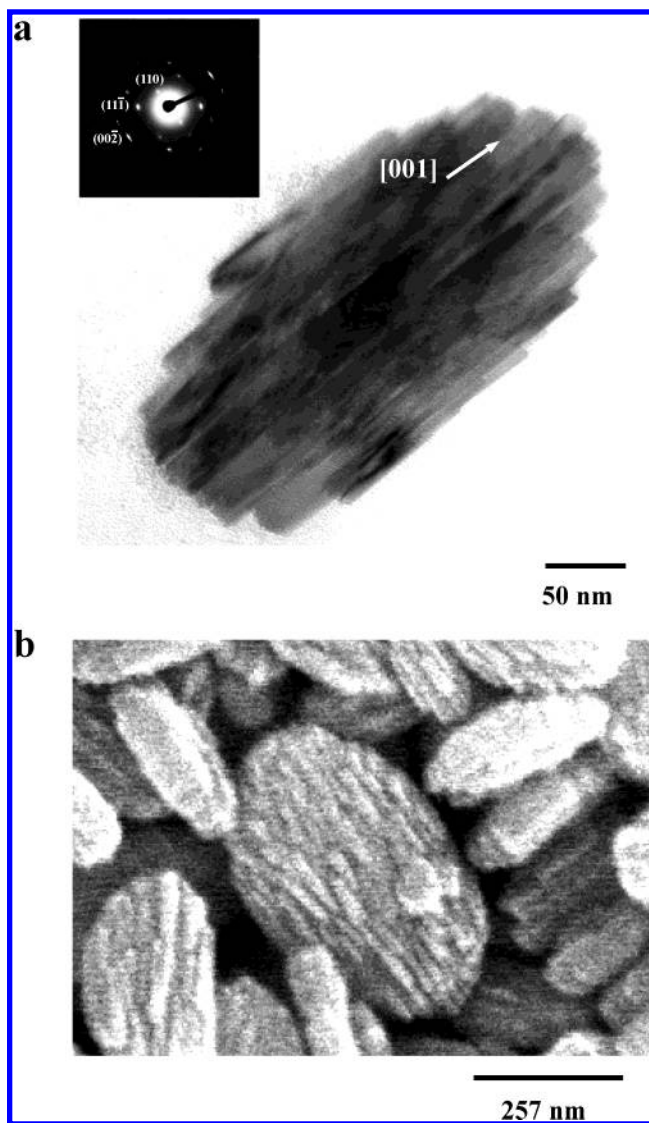


Figure 5. (a) Higher magnification of TEM image for a single GaOOH crystal. The inset displays the corresponding electron diffraction pattern. (b) SEM image of the GaOOH crystals. A 1064 nm wavelength using 100 mJ/pulse for a 20 min exposure time was used to prepare samples with the presence of 2.2×10^{-3} M CTAB. Both (a) and (b) crystals were attained via a course of aging 7 days.

On the other hand, the resulting solutions containing SDS or pure water did not yield those spindle structures as exclusively observed in CTAB. Following the same scenario in CTAB, three different SDS concentrations, i.e., 5×10^{-3} M (below cmc), 1×10^{-2} M (near cmc), and 2×10^{-2} M (above cmc), were prepared to study the effect in forming gallium-based materials. XRD measurements determined the amorphous structure, except for a couple of peaks which were equivocally attributed to $\beta\text{-Ga}_2\text{O}_3$ due to poor signal-to-noise. Figure 4a displays the typical morphology attained from 1×10^{-2} M of SDS circumstance, where the product was aged for 7 days. In pure water, the resulting species mostly manifested a fluffy aggregate, but the ellipsoidal particles could be occasionally observed, as depicted in Figure 4b. Interestingly, some GaOOH diffraction peaks corresponding to (110), (130), (040), (111), and (221) accompanied with a broad background between 20° and 40° (2θ) in XRD. Such results suggest that the materials prepared from pure water consisted of GaOOH and amorphous structures.

Figure 5a exhibits higher magnification of TEM image for a single GaOOH crystal. As seen in the image, the spindle-like GaOOH formed a type of layered structure. The inset shows

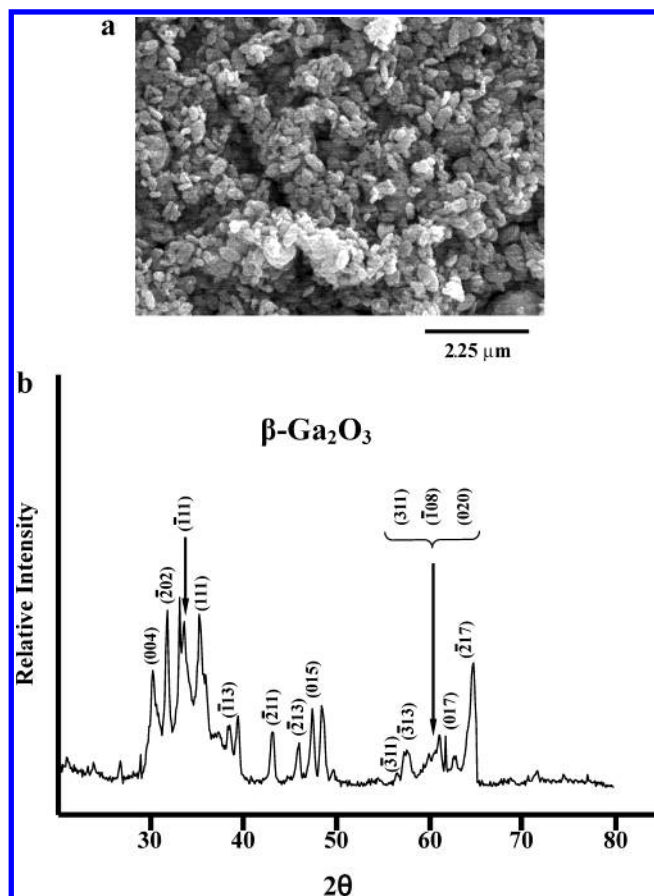


Figure 6. (a) SEM image of sample calcined at 750 °C for 18 h. (b) The corresponding XRD spectrum showing β -Ga₂O₃ patterns after 750 °C calcination for 18 h. A 1064 nm wavelength using 100 mJ/pulse for a 20 min exposure time was introduced to prepare samples with the presence of 2.2×10^{-3} M CTAB. The ellipsoidal GaOOH crystals after aging 7 days were used to perform calcination.

the corresponding electron diffraction pattern with an incident electron beam along the $[1\bar{1}0]$ direction. It indicates axial direction as (110) plane for ellipsoidal morphology and grew along the $\langle 001 \rangle$ axis. The SEM image of Figure 5b clearly displays the striped texture of the as-prepared GaOOH. GaOOH had previously been designated as a diaspor structure, consist-

ing of double chains of an edge-shared octahedron. Gallium atoms occupy octahedral sites, surrounded by six oxygens, and each oxygen is linked to three gallium atoms.^{21,22,26}

The spindle-like GaOOH, which was attained after aging 7 days, was further studied by a calcination process. Figure 6a illustrates the morphology of GaOOH particles after calcination at 750 °C for 18 h. Although some particles exhibit fusion behavior, most of them retained an ellipsoidal structure. The XRD patterns show that these crystals transformed from GaOOH to β -Ga₂O₃, as seen in Figure 6b. On the other hand, α -Ga₂O₃ structure was attained if calcination was conducted in a stepwise operation. The dominant peaks of the XRD spectrum were identified as α -Ga₂O₃. The ellipsoidal GaOOH was calcined in the following procedure: 250 °C for 64 h \rightarrow 250 °C for 64 h \rightarrow 750 °C for 18 h. Once again, most of the crystals α -Ga₂O₃ preserved the same ellipsoidal morphology as those observed in Figure 6a. In this stepwise pathway, two consecutive calcination processes at 250 °C were conducted. We have investigated the crystal structures after consecutive calcination at 250 °C. Interestingly, XRD measurements indicated that those calcined crystals retained the GaOOH patterns. In contrast to the calcination behavior studied by Tas et al., their synthesized nano- and micro-GaOOH transformed to α -Ga₂O₃ at 500 °C and converted into β -Ga₂O₃ at a temperature of 750 °C.²²

In the studies of nanoparticles form a metal bulk via laser ablation, Kondow and co-workers investigated several metal nanoparticles and postulated a dynamic formation mechanism.^{3–6} A metal plume was developed over the laser spot, where the metal plate was irradiated by laser. The metal atoms or small clusters constituting the metal plume would rapidly aggregate for the further growth process. In our case, the structureless embryos containing gallium were generated immediately after laser ablation operation, followed by a slow crystallization process via aging with the aid of CTAB surfactant. As mentioned above, CTAB particularly facilitated spindle-like GaOOH formation. The nascent colloidal solution, immediately after laser ablation, was utilized for ζ -potential measurements. To clarify the role of CTAB, the ζ -potential of the nascent product in a native form (without surfactants) was performed. The ζ -potential was determined as -23 mV. The negative value clearly indicates the negatively charged surface of the gallium-based amorphous hydroxide and explicates the positively

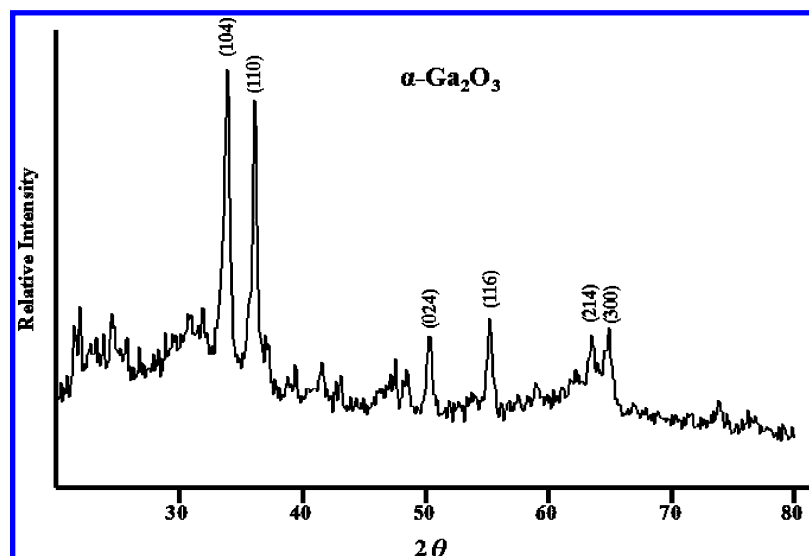


Figure 7. XRD spectrum showing α -Ga₂O₃ patterns via a stepwise calcination: 250 °C (64 h) \rightarrow 250 °C (64 h) \rightarrow 750 °C (18 h). A 1064 nm wavelength using 100 mJ/pulse for a 20 min exposure time was introduced to prepare a sample with the presence of 2.2×10^{-3} M CTAB. The ellipsoidal GaOOH crystals after aging 14 days were used to study calcination behavior.

charged CTAB adsorbed electrostatically via the headgroup $^+\text{N}(\text{CH}_3)_3(\text{C}_{16}\text{H}_{33})$ on the negatively charged surface. As the experimental results shown, the ellipsoidal structure can be readily formed in below, near, or above cmc of CTAB. Although the detailed surfactant-assisted formation mechanism remains to be resolved, it is postulated that CTAB might have stabilized the laser-generated particle embryos and clusters allowing further condensation to give final ellipsoidal nanocrystals. On the basis of HRTEM (Figure 5a), cationic CTAB possibly interacted preferentially with the [001] surfaces, leading to develop along these surfaces. Preliminary attempts by replacing $\text{C}_{16}\text{H}_{33}\text{N}(\text{CH}_3)_3\text{Br}$ (CTAB) with $(\text{CH}_3)_4\text{N}^+\text{OH}^-$ (2.2×10^{-3} M) demonstrated that $(\text{CH}_3)_4\text{N}^+$ with shorter carbon chain also formed the ellipsoidal particles. The effect of the chain length in surfactant needs to be further investigated in details. Finally, the ellipsoidal GaOOH nanocrystals were found to crystallize slowly in the aging process. Such a slow crystallization course is not clear, although we have inspected formation features as a function of the aging period. TEM images showed that the resulting precipitates formed as the fluffy aggregates accompanied with the spherical-like particles after 30, 60, 80, 110, and 135 min of aging. No distinct morphology could be observed from these several time intervals. However, the long time of formation could possibly result from the growth of the gallium-based particles occurred by diffusion of solute species to the particles and transformed into ellipsoidal GaOOH through a dissolution recrystallization process.²⁷

Conclusions

In addition to forming pure metal nanoparticles, this study demonstrated that laser ablation methodology can be applied to prepare metal hydroxide or oxide species. Interestingly, the nature of the surfactants strongly affected GaOOH crystallization. The spindle-like GaOOH can be readily formed with the presence of cationic CTAB surfactant. Furthermore, the different calcination behavior up to 750 °C determined α - or β -Ga₂O₃ formation. The optical properties of as-prepared gallium oxides are under investigation.

Acknowledgment. We thank the National Science Council of the Republic of China for financially supporting this work. We also acknowledge Ms. H. J. Shih for the SEM images, Mr. R. C. Lee for the XPS determination, and Ms. S. Y. Hsu and

Mr. S. Y. Yao for the TEM measurements at Taiwan Regional Instrument Center, National Cheng Kung University.

References and Notes

- (1) Fojtik, A.; Henglin, A. *Ber. Bunsen-Ges. Phys. Chem.* **1993**, *97*, 252.
- (2) Sibbald, M. S.; Chumanov, G.; Cotton, T. M. *J. Phys. Chem.* **1996**, *100*, 4672.
- (3) Mafuné, F.; Kohno, J.; Jakeda, Y.; Kondow, T.; Sawabe, H. *J. Phys. Chem. B* **2000**, *104*, 9111.
- (4) Mafuné, F.; Kohno, J.; Jakeda, Y.; Kondow, T.; Sawabe, H. *J. Phys. Chem. B* **2000**, *104*, 8333.
- (5) Mafuné, F.; Kohno, J.; Jakeda, Y.; Kondow, T.; Sawabe, H. *J. Phys. Chem. B* **2001**, *105*, 9050.
- (6) Mafuné, F.; Kohno, J.; Jakeda, Y.; Kondow, T. *J. Phys. Chem. B* **2003**, *107*, 4218.
- (7) Yeh, Y. H.; Yeh, M. S.; Lee, Y. P.; Yeh, C. S. *Chem. Lett.* **1998**, 1183.
- (8) Yeh, M. S.; Yeh, Y. S.; Lee, Y. P.; Lee, H. F.; Yeh, Y. H.; Yeh, C. S. *J. Phys. Chem. B* **1999**, *103*, 6851.
- (9) Lee, Y. P.; Liu, Y. H.; Yeh, C. S. *Phys. Chem. Chem. Phys.* **1999**, *1*, 4681.
- (10) Kao, H. M.; Wu, R. R.; Chen, T. Y.; Chen, Y. H.; Yeh, C. S. *J. Mater. Chem.* **2000**, *10*, 2802.
- (11) Chen, Y. H.; Yeh, C. S. *Colloids Surf. A* **2002**, *197*, 133.
- (12) Chen, T. Y.; Chen, S. F.; Sheu, H. S.; Yeh, C. S. *J. Phys. Chem. B* **2002**, *106*, 9717.
- (13) Chen, S. F.; Yeh, C. S. *J. Chin. Chem. Soc.* **2002**, *49*, 895.
- (14) Kabashin, A. V.; Meunier, M.; Kingston, C.; Luong, J. H. T. *J. Phys. Chem. B* **2003**, *107*, 4527.
- (15) Zhang, J.; Worley, J.; Dénommée, S.; Kingston, C.; Jakubek, Z. J.; Deslandes, Y.; Post, M.; Simard, B.; Braid, N.; Botton, G. A. *J. Phys. Chem. B* **2003**, *107*, 6920.
- (16) Binet, L.; Gourier, D. *J. Phys. Chem. Solids* **1998**, *59*, 1241.
- (17) Choi, Y. C.; Kim, W. S.; Perk, Y. S.; Lee, S. M.; Bae, D. J.; Lee, Y. H.; Perk, G. S.; Choi, W. B.; Lee, N. S.; Kim, J. M. *Adv. Mater.* **2000**, *12*, 746.
- (18) Hu, J. Q.; Li, Q.; Meeng, X. M.; Lee, C. S.; Lee, S. T. *J. Phys. Chem. B* **2002**, *106*, 9536.
- (19) Edwards, D. D.; Mason, T. O.; Goutenoire, F.; Poeppelmeier, K. R. *Appl. Phys. Lett.* **1997**, *70*, 1706.
- (20) Ueda, N.; Hosono, H.; Waseda, R.; Kawazoe, H. *Appl. Phys. Lett.* **1997**, *71*, 933.
- (21) Avivi, S.; Mastai, Y.; Hodes, G.; Gedanken, A. *J. Am. Chem. Soc.* **1999**, *121*, 4196.
- (22) Tas, A. C.; Majewski, P. J.; Aldinger, F. *J. Am. Ceram. Soc.* **2002**, *85*, 1421.
- (23) Cifuentes, A.; Bernal, J. L.; Diez-Masa, J. C. *Anal. Chem.* **1997**, *69*, 4271.
- (24) Sato, T.; Nakamura, T. *J. Chem. Technol. Biotechnol.* **1982**, *21*, 469.
- (25) Li, H.; Tripp, C. P. *Langmuir* **2002**, *18*, 9441.
- (26) Hu, Y.; Liu, X. Z. *Miner. Eng.* **2003**, *16*, 219.
- (27) Morales, M. P.; González-Carreño, T.; Serna, C. J. *J. Mater. Res.* **1992**, *7*, 2538.